Electronic Supplementary Information (ESI)

Saponin-containing multifunctional binder toward superior long-cycling stability in Li-S batteries

*Soochan Kim, Misuk Cho, and Youngkwan Lee**

School of Chemical Engineering, Sungkyunkwan University, Suwon 16419, Republic of Korea
E-mail: yklee@skku.edu

Experimental Section

Materials

Saponin was purchased from the Tokyo Chemical industry CO., LTD (Japan). Sulfur, lithium metal, bis(trifluoromethyl sulfonyl)amine lithium salt (LiTFSI), 1,3-dioxolane (DOL), dimethoxyethane (DME), Poly(acrylic acid) (PAA) (M_v 450,000 g mol^{-1}), Triton X-100, and cetyltrimethylammonium bromide (CTAB) were purchased from Sigma-Aldrich (USA). Lithium nitrate ($LiNO_3$) and Li_2S were purchased from Alfa Aesar (USA).

Material characterization

The zeta potential of carbon black was determined using a zeta meter (ELS-Z, Otsuka Electronics, Japan). The surface morphology and elemental dispersive analysis on the cathode were observed by SEM (JSM-6390A, JEOL, Japan). EIS was performed with a potentiostat (VSP, BioLogic, France). The LPS absorption capability was evaluated by UV–Vis spectroscopy (8453 UV–Vis Spectroscopy System, Agilent, USA). The local mechanical properties were investigated by nano-indentation with a 0.5 μm 90° Conical indenter (NanoTest NTX, Micro Materials, UK). Ketjen black (KJB, EC-600JD) was purchased from Akzo Nobel (the Netherlands), and carbon black was purchased from Wellcos (Republic of Korea).

Electrochemical characterization

Electrochemical characterization was carried out in a CR2032-type coin-cell. To prepare the sulfur cathode, sulfur/KJB composites (7/3, w/w), carbon black, 5 wt.% PAA (in deionized water), and additives (saponin, Triton X-100, or CTAB) were mixed in a weight ratio of 8:1:1 (sulfur composites: carbon black: binder). The amounts of additives were controlled from 0.5 to 2 wt.% of the whole weight of the cathode slurry. Subsequently, the mixed slurry was

homogeneously coated onto an aluminum foil (thickness: 20 μm) using a doctor blade. Finally, the electrodes were dried at 50 °C in the atmosphere for 12 h, and at 50 °C in a vacuum oven for 6 h. For heat-treated saponin additives (HT-Saponin), the dried electrode was heated for 15 min at 120 °C in a convection oven. The typical loading of sulfur was approximately (0.8–1.0) mg cm^{-2}. For a high sulfur loading, the cathodes were fabricated on carbon paper (AvCarb, Ballard, USA), using a similar procedure to that described above. The electrolyte was a mixture of DOL and DME (1:1, v/v) with 1 M LiTFSI and 0.2 M $LiNO_3$. The Li–S cells were assembled in a 2032 type coin-cell using the sulfur electrode as a working electrode, lithium metal as the counter electrode, and Celgard membrane (2400) as the separator, in an Ar-filled glove box containing less than 10 ppm of both H_2O and O_2. The galvanostatic discharge–charge behaviors were monitored using a battery test system (WonATech Corp., Republic of Korea) with a voltage range of (1.7–2.8) V vs. Li/Li^+ at 25 °C, and all the Li–S cells were activated at 0.05 C for 2 cycles prior to measurements. EIS measurements were conducted using a potentiostat (VSP, BioLogic, France), applying a 50 mV amplitude sine wave in the frequency range of 0.1 Hz to 100 kHz. To measure the ionic conductivity of polymer films, the 2032 type coin-cell (stainless//polymer film//stainless) was assembled and evaluated by using EIS in the frequency range from 100 kHz to 1 Hz at temperatures at 25 °C for 5 times, repeatedly.

Synthesis of sulfur/KJB composites

To synthesize the S/KJB composite, sulfur and KJB were mixed at a mass ratio of 7:3. The mixture was then heated at 155 °C for 15 h under Ar atmosphere, in order to melt sulfur into the pores in carbon matrix.

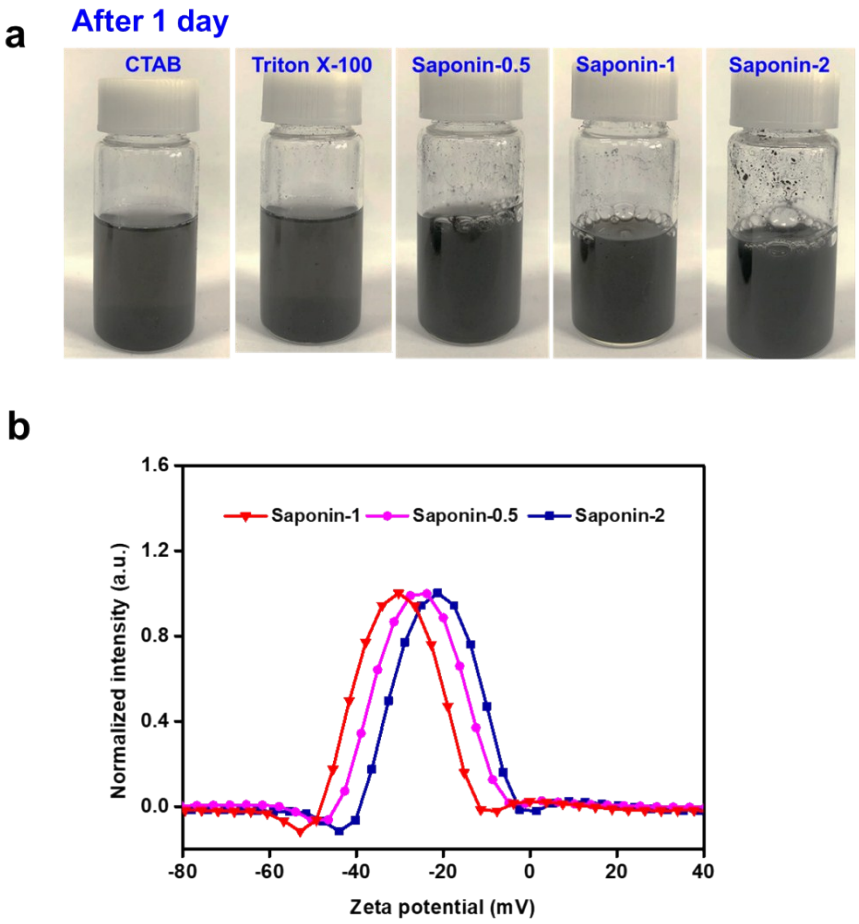

Fig. S1. (a) optical images after mixing to see the stability of dispersion (b) Zeta potentials of carbon black according to various concentration of saponin.

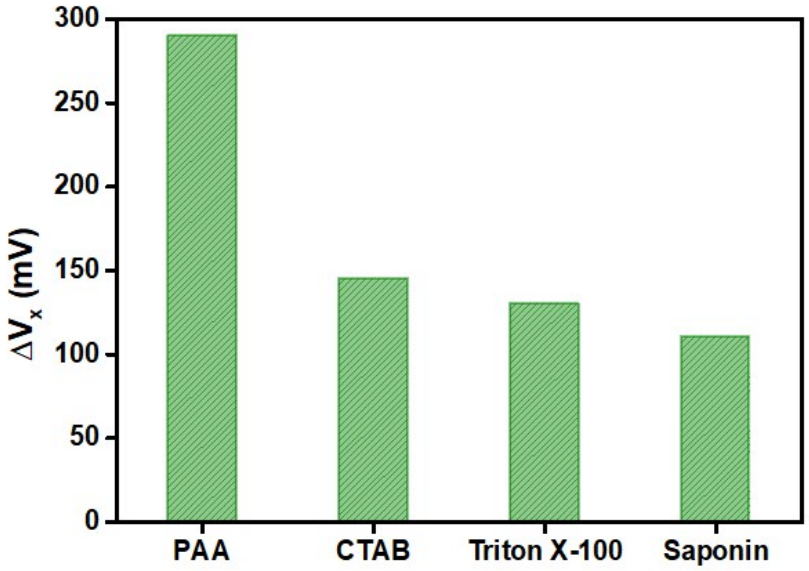

Fig. S2. The voltage difference between the charge and discharge plateau of prepared Li-S cells

The voltage difference (ΔV_X) between the charge and discharge plateau shows the polarization and roundtrip energy efficiency of cell. Lower polarization (lower voltage difference) represents a more kinetically efficient reaction process with smaller barrier.[S1,S2]

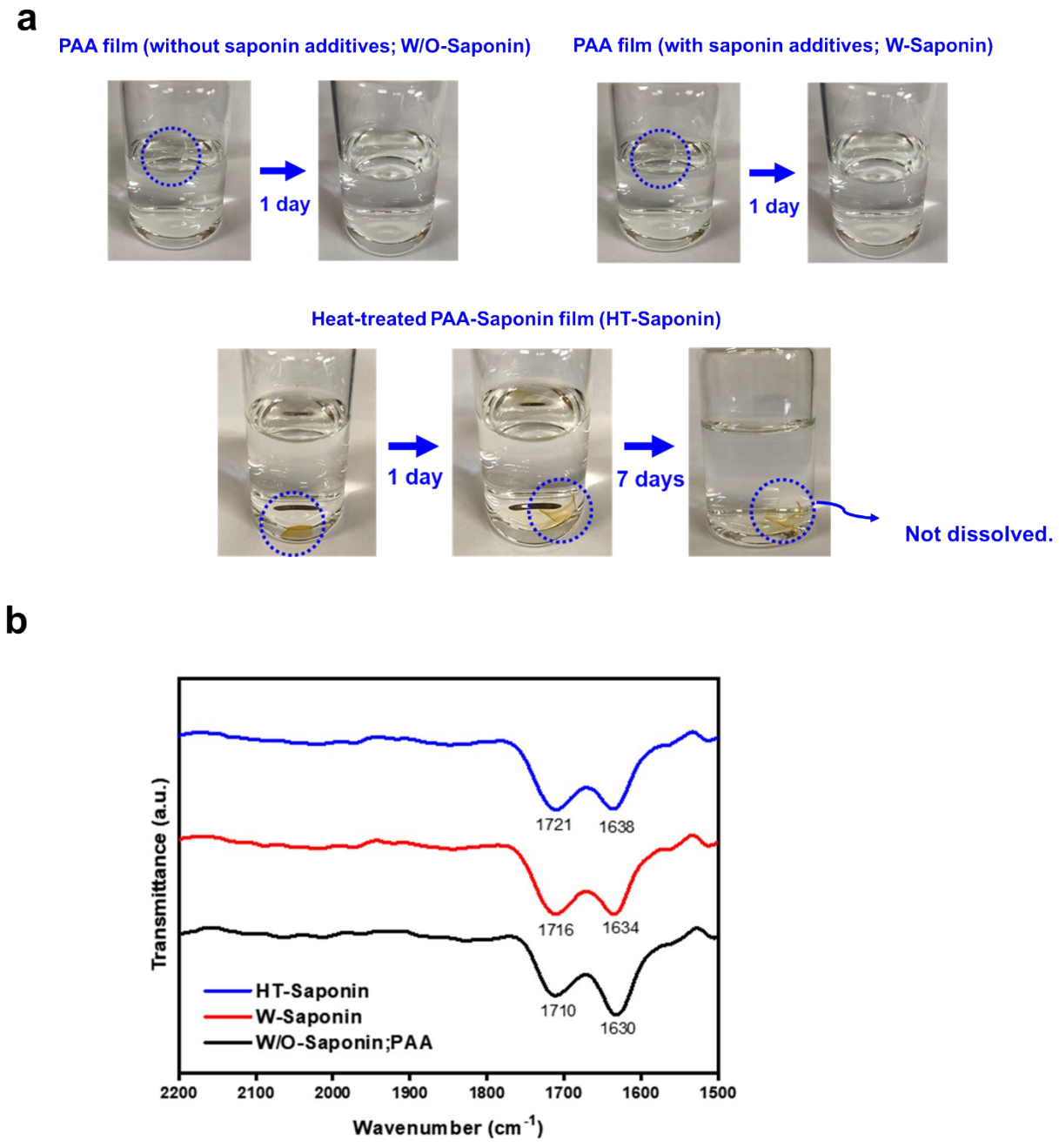

Fig. S3. (a) optical images of PAA film (W/O-Saponin), PAA film with saponin (W-Saponin), and heat-treated PAA film with saponin (HT-Saponin) and (b) FT-IR spectra of samples (W/O-Saponin, W-Saponin, and HT-Saponin)

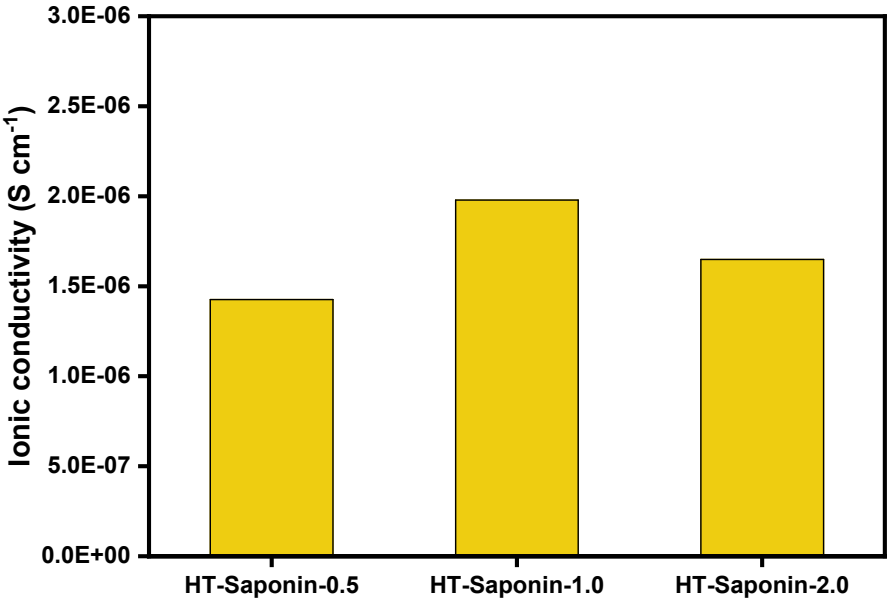

Fig. S4. Ionic conductivity of prepared polymer films at 25 °C from EIS (electrochemical impedance spectroscopy).

Ionic conductivity at 25 °C: 0.5 wt.% of saponin, 1.4 x 10^{-6} S cm^{-1}; and 2 wt.% of saponin, 1.6 x 10^{-6} S cm^{-1}. Each polymer film was sandwiched between a stainless steel (SS) disc (d = 1.6 cm) in the 2032 type coin cell. The cell was sealed to prevent contamination from oxygen, moisture, and other substances in glove box under Ar atmosphere. The ionic conductivity was calculated from the electrolyte resistance (*R*s) obtained from the intercept of the AC impedance spectra with the real axis, the film thickness (*l*, ~50 μm), and the electrode area (A, 2 cm^2) by the equation 1.[S3]

$$\sigma\ (Ionic\ conductivity) = \frac{l}{Rs \times A} \quad \cdots\cdots\cdots\cdots \text{(Equation 1)}$$

Saponin has unique amphiphilic structure with hydrophilic glycosides and hydrophobic aglycone. According to the reported researches, glycosides-based materials, like as polysaccharides which have abundant ether groups (-C-O-C-) with that of poly(ethylene oxide), could present the ability to disaggregate lithium salts, adsorb the organic solvents, and promote the migration of lithium ions.[S4, S5] Therefore, the adding of saponin can increase the

ionic conductivity.

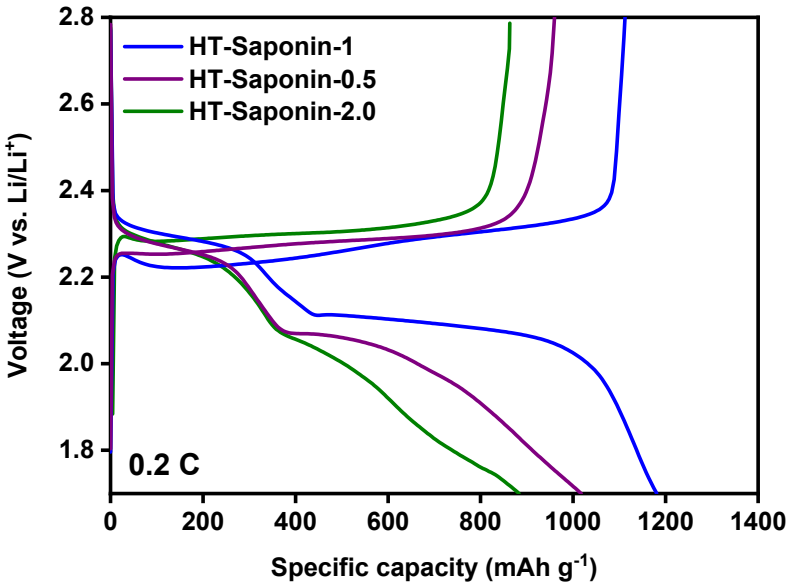

Fig. S5. Galvanostatic charge-discharge profiles of prepared Li-S cells at 0.2 C (after activation)

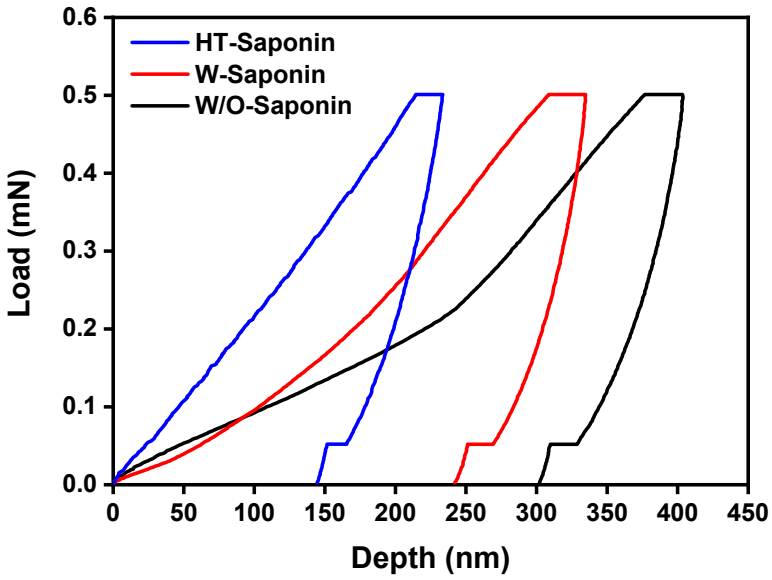

Fig. S6. Local mechanical properties of the before cycled Li–S cathode obtained by nanoindentation tests: Representative load–displacement curves for Li–S cathodes.

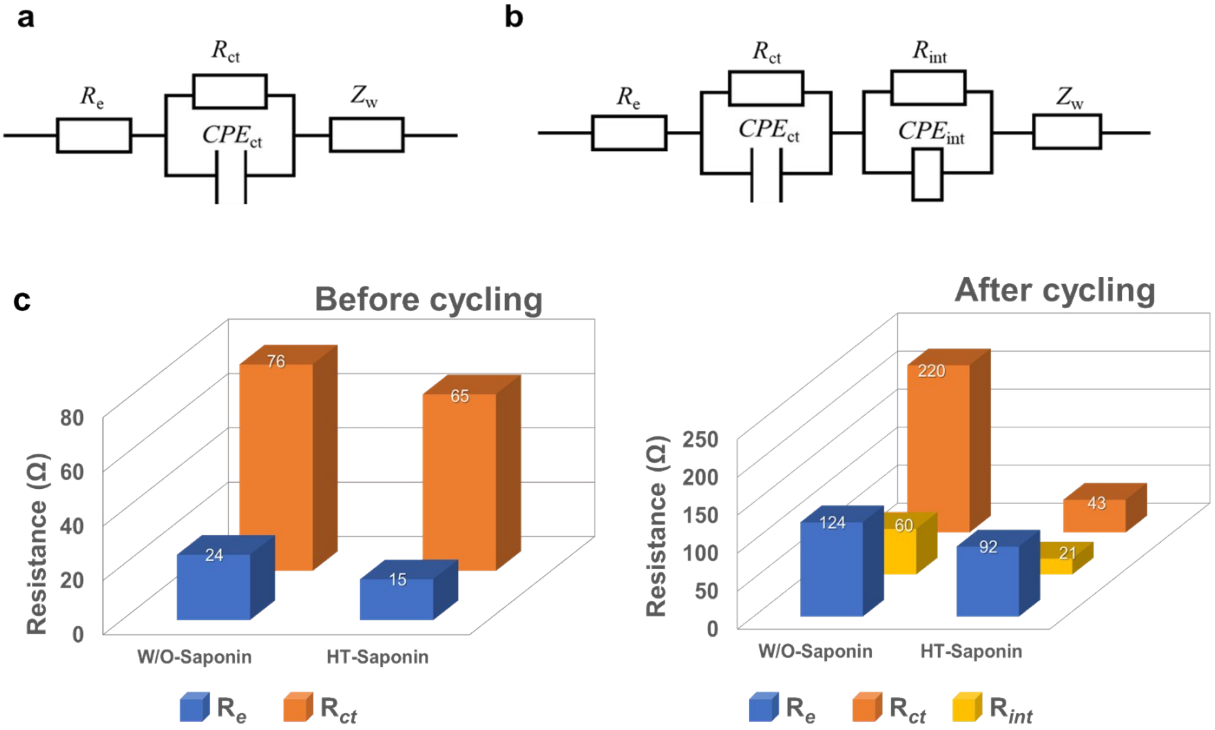

Fig. S7. EIS circuits. (a) for EIS analysis before cycling and (b) for EIS analysis after charging-discharging 100 cycles. (c) detailed EIS results of Fig. 4a-b.

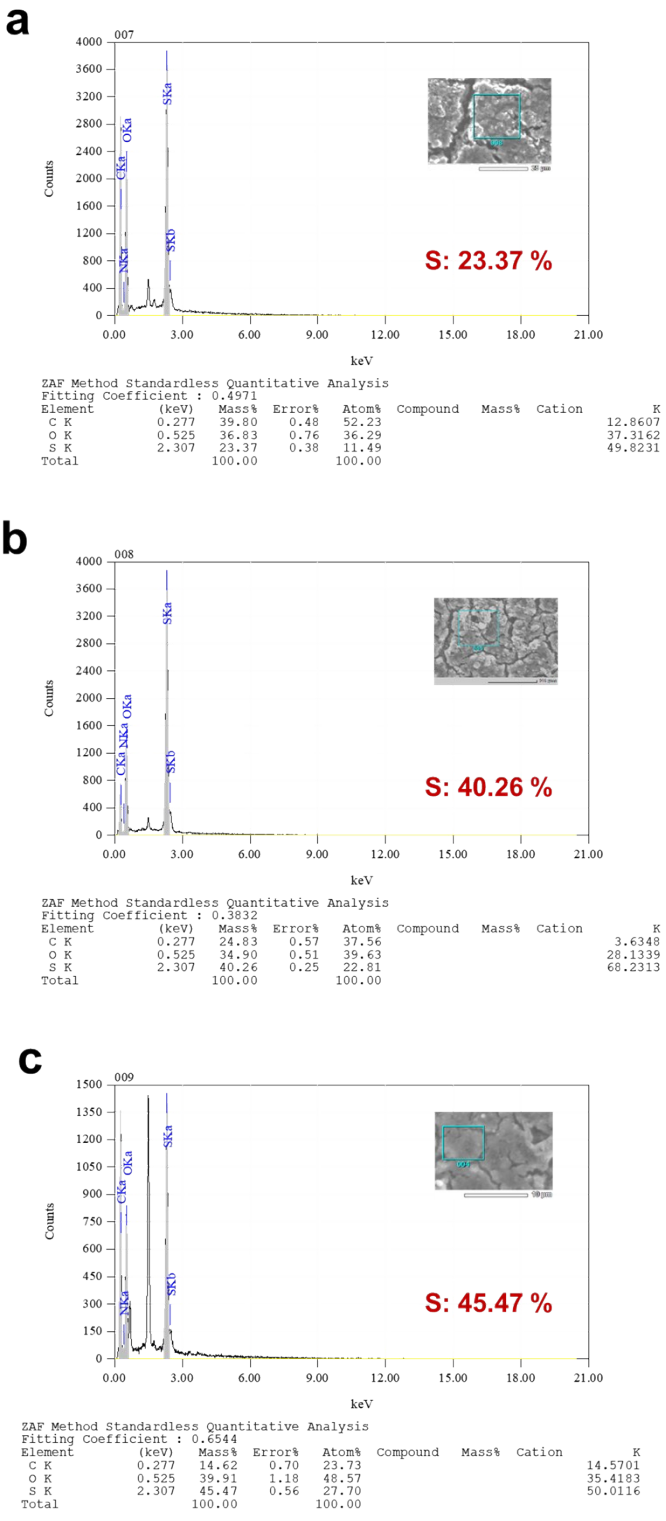

Fig. S8. EDX results of Li-S cathode without saponin (a), with saponin (b), and with HT-Saponin (c) after 100 cycles.

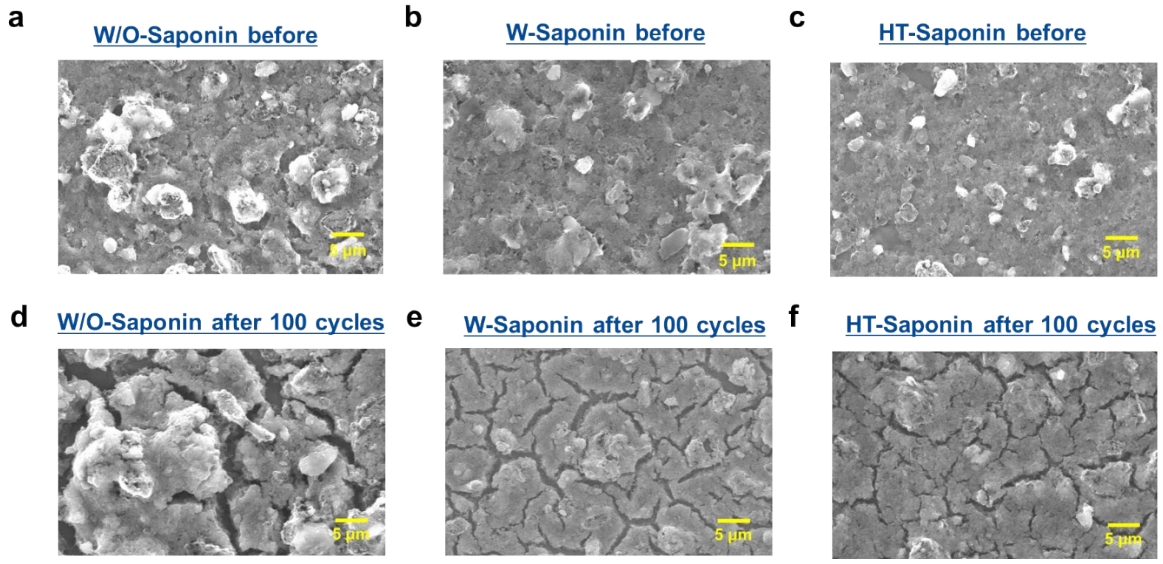

Fig. S9. SEM images of prepared Li-S cathodes (before and after 100cycles, scale bar; 5 µM)

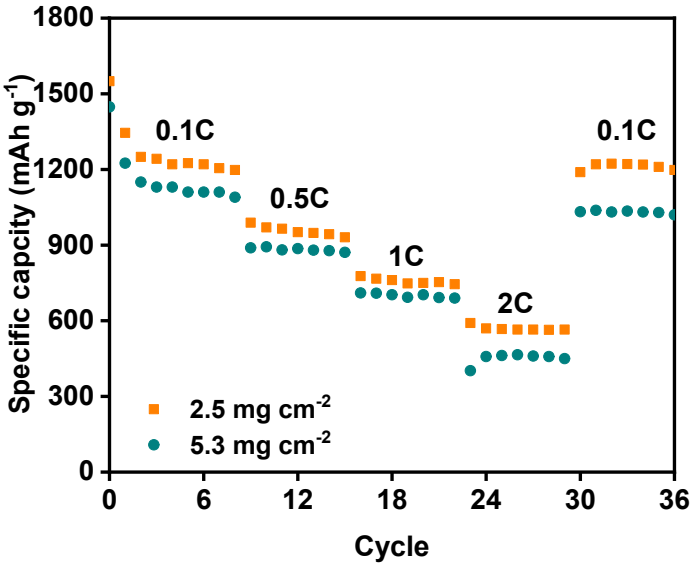

Fig. S10. Rate capability test of the Li–S cell at 0.1, 0.5, 1, and 2C.

Table S1. Comparison of battery performance and the stability of Li–S cells using various additives.

Additives (amounts of additives)	**Initial discharging capacity (mAh g^{-1})**	**Final discharging capacity (mAh g^{-1})**	**Cycle**	**Capacity decay (%) per cycle**	**Rate**	**Ref.**
Cu powder (26%)	1500 at 0.1C	1300	80	0.167	0.1	**[S6]**
Black $BaTiO_3$ (10%)	1129 at 0.1C	681.9	200	0.099	0.5	**[S7]**
MgO (10%)	900 at 0.2C	750	100	0.083	0.2	**[S8]**
Nano-Aluminum (1.13%)	978 at 0.2C	698	300	0.096	0.2C	**[S9]**
TiS_2 (9%)	~1050 at 0.05C	500	250	0.114	0.2C	**[S10]**
$Fe_{1-X}S$ (15%)	1000 at 0.2C	800	300	0.067	0.2	**[S11]**
$Mg_{0.6}Ni_{0.4}O$ (20%)	1223 at 0.05C	1100	100	0.1	0.1	**[S12]**
HT-Saponin (1%)	**1498 at 0.05C**	**638**	**1,000**	**0.012**	**2 C**	**Our work**

References

S1.J. Yan, X. Liu, and B. Li, *Adv. Sci*., 2016, **3**, 1600101.

S2.F. Pei, L. Lin, D. Ou, Z. Zheng, S. Mo, X. Fang, and N. Zheng, *Nat. Commun*., 2017, **8**, 482.

S3.J. Lee, S. Kim, M.Cho, C. Chanthad, and Y. Lee, *J. Electrochem. Soc.*, 2019, **166**, A2755.

S4.D. Xu, J. Jin, C. Chen, and Z. Wen, *ACS Appl. Mater. Interfaces*, 2018, **10**, 38526-38537.

S5.D. Xu, B. Wang, Q. Wang, S. Gu, W. Li, J. Jin, C. Chen, and Z. Wen, *ACS Appl. Mater. Interfaces,* 2018, **10**, 17809-17819.

S6.L. Jia, T. Wu, J. Lu, L. Ma, W. Zhu and X. Qiu, *ACS Appl. Mater. Interfaces*, 2016, **8**, 30248-30255.

S7.Z. Zhao, G. Li, Z. Wang, M. Feng, M. Sun, X. Xue, R. Liu, H. Jia, Z. Wang, W. Zhang, H. Li and Z. Chen*, J. Power Sources*, 2019, **434**, 226729.

S8.R. Ponraj, A. G. Kannan, J. H. Ahn and D.-W. Kim, *ACS Appl. Mater. Interfaces*, 2016, **8**, 4000-4006.

S7.Y. Zhao, M. Yu, D. Wang, J. Ma, W. Gong and H. Qiu, *J. Electroanal. Chem.*, 2019, **837**, 116-122.

S9.K. Sun, M. Fu, Z. Xie, D. Su, H. Zhong, J. Bai, E. Dooryhee and H. Gan, *Electrochim. Acta*, 2018, **292**, 779-788.

S10.J. H. Ahn, G. K. Veerasubramani, S.-M. Lee, T.-S. You and D. -W. Kim, *J. Electrochem. Soc.*, 2018, **166**, A5201.

S11.Y. Zhang, Y. Zhao, A. Yermukhambetova, Z. Bakenov and P. Chen, *J. Mater. Chem. A*, 2013, **1**, 295-301.